CEB, COMITÉ EURO INTERNACIONAL DU BÉTON

RTU, RIGA TECHNICAL UNIVERSITY

INTERNACIONAL CONFERENCE

BOND IN CONCRETE

FROM RESEARCH TO PRACTICE

PROCEEDINGS
TOPICS
7-12

RIGA, LATVIA, OCTOBER 15-17, 1992

BOND-SLIP-STRAIN RELATIONSHIP OF DEFORMED BARS

Hiroshi SHIMA
Associate professor
University of Tokushima
Tokushima, Japan

Lie-Liung CHOU
Chief engineer
Taipei Railway Underground Project
Republic of China

Hajime OKAMURA
Professor
University of Tokyo
Tokyo, Japan

ABSTRACT

It was clarified that the bond stress-slip relationship was not unique but the bond stress-slip-strain relationship was unique under different boundary conditions. Bond tests of deformed bars embedded in massive concrete which have no effect of splitting crack were carried out. The bond-slip relationships obtained from extremely short embedded specimens are different from those obtained from longer ones. In the cases of short embedded pull-out test and short embedded axial tension test, the bond-slip relationships are different according to the location along a bar. The bond-slip relationship of an aluminum bar is different from that of steel bar. The bond stress decreased so much after yielding of steel bar. These results can be explained by the proposed unique bond-slip-strain relationship.

Key-words: bond-slip-strain model, bond-slip relationship, strain, post-yield range, deformed bar

1. INTRODUCTION

In the analysis of reinforced concrete structures, bond action between steel bars and concrete is often considered by using a bond-slip relationship. The bond-slip relationship expresses the local bond stress at any location along a bar as a function of the local slip. Many bond-slip relationships have been published and some of them were formulated, but they are very different each other as shown in Fig.1 because bond-slip relationships are affected by various factors which are different in each bond test.

Bond-slip relationships utilized in the analysis of reinforced concrete structures are generally derived based on results of bond tests. Most of those relationships were obtained from specimens with short length using the average bond stress /2,4,5/. Therefore, it is unreasonable to apply these models to actual members which usually have large embedment length. Therefore, more realistic bond-slip relationship which expresses the difference caused by embedment length or location along a bar should be developed.

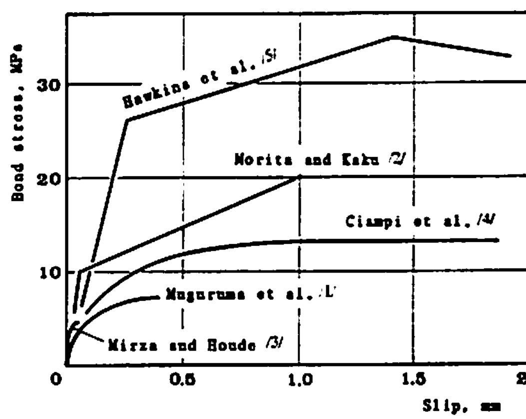

Fig.1 Comparison of previously proposed bond-slip models

Regarding to the effect of steel stress on bond for deformed bars, it has been considered that the stress in a bar does not affect the bond stress because the bond of a deformed bar depends on the mechanical action of ribs rather than on the friction as in the case of plain bars.

This paper describes the mechanism of these differences in bond-slip relationship by taking account of the effect of steel strain on the relationship. Bond stress at any location along a bar is expressed by an unique bond-slip-strain relationship even under different embedment lengths or different boundary conditions.

2. EXPERIMENTS

2.1 Specimen and Experimental Conditions

Both pullout and axial tension tests were carried out. The specimen for the pullout is shown in Fig.2. A steel bar was arranged vertically in the center of a concrete cylindrical specimen having diameter of 50cm. This diameter was determined to be large enough to prohibit a splitting crack and to make stress in concrete small and uniform. The experimental conditions and properties of each specimen are shown in Table 1. The following five series of tests were carried out.

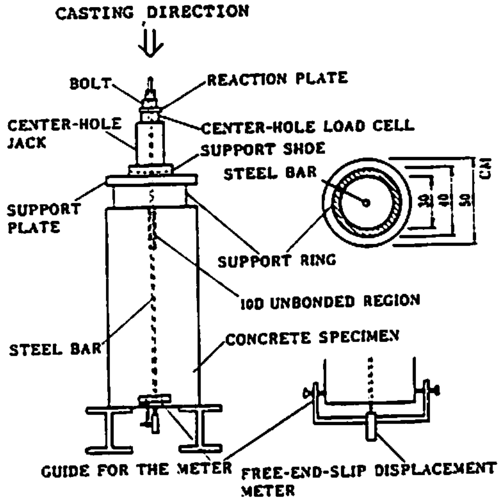

Fig.2 Specimen and apparatus for pullout test.

(1) Series I consists of pullout tests in which embedded lengths were shortened and varied to obtain various free end slips with zero-stress of the bar. In a part of this series, unbonded length at the free end is varied in order to check the effect of end block at the free end. (2) Series II is an axial tension test in which the length of the specimen is selected to be 40*D* (*D*: nominal diameter of the bar), to make the bar at the center of the specimen have some stress where the slip is zero. (3) Pull-out bond tests using an aluminium bar which had smaller Young's modulus than that of steel was carried out in Series III to investigate the effect of strains on bond-slip relationships.' (4) Series IV consists of pullout tests in which embedded lengths are extremely short to investigate the influence of concrete strength where the strain is very small while the slip is large. (5) Specimens in Series V have long embedded lengths such as 40*D* or 50*D* to get zero-stress with zero-slip. The effect of bar diameter and strength of concrete on bond-slip relationships are investigated.

Table 1 Properties of specimens.

Series	Specimen No.	D (mm)	f'c (MPa)	E.L. (D)	U.L.L. (D)	U.L.F. (D)	Remarks
I	1 2 3 4 5 6	25.4*	21.8	5 10 15 20 30 40	0	0	Embedded length of bars
	7 8 9	30.7	18.5	6	10	0 2.5 5.0	Unbonded length at free end
II	10	19.5*	21.6	40	10	0	Axial tension test
III	11 12	17.7*	34.3	40	10	0	Steel Aluminium
IV	13 14 15	30.7	18.5 33.0 38.7	2	10	0	Strength of concrete
V	16 17 18	25.4	22.4 27.2 50.0	40	0	0	Strength of concrete
	19 20 21	19.5* 25.4* 30.7*	21.2	50	0	0	Diameter of bars

D: Diameter of bar (*: Heat treatment)
f'c: Compressive strength of concrete, Max size of aggregate was 25mm
E.L.: Embedded length
U.L.L.: Unbonded length at loaded end
U.L.F.: Unbonded length at free end

2.2 Properties of Bars

The measurement of steel strain along a bar is the most important work in the experiment, because the local bond stress and slip are determined by strain distribution along the bar. If ordinary steel bars were used, ribs of the bar should have been removed to attach strain gauges resulting in reduction of the cross-sectional area of the bar. To solve this problem, screw-shaped deformed bars without longitudinal ribs were used. The bar sizes were D19, D25 and D32. Aluminium and steel bars used in Series III were machined so that the distance and geometry of the ribs became similar to D19 bar used in other series. The dimensions and properties of bars are given in Table 2.

Table 2 *Properties and dimensions of bars.*

Type of bar	D32	D25	D19	Steel	Aluminium
Nominal diameter, mm	31.8	25.4	19.1	—	—
Nominal curcumference, cm	10.0	8.0	6.0	—	—
Diameter for analysis, mm	30.7	25.4	19.5	19.5	19.5
Area for analysis, cm^2	7.40	5.06	2.98	2.98	2.98
Lug spacing, mm	16.6	13.9	9.9	9.9	9.9
Lug height, mm	2.1	1.8	1.5	1.5	1.5
Projected length of lug*1, cm	7.0	5.4	3.6	3.6	3.6
Bearing area of lug*2, mm^2	146	98	54	54	54
Bearing area coefficient, %	8.8	8.8	9.1	9.1	9.1
Yield point, MPa	336*3	428*3	366*3	480	450*4
Young's modulus, GPa	190	190	190	190	72

*1 Length of a lug projected on plane perpendicular to bar axis
*2 Bearing area of a lug projected on plane perpendicular to bar axis
*3 Before heat treatment
*4 Elastic limit

High strength steel bars were used to obtain large slips even before the yielding of steel, because the slips of ordinal strength steel bars could not be large. The high strength steel bars were obtained by a special heat treatment of ordinary steel bars.

2.3 Description of Test

Foil resistance strain gauges having gauge length of 5mm were attached on opposite faces at basically an interval of *5D*. The gauge interval of Specimens No.7 to No.9 was *2D* because these specimens were aimed to investigate the bond behaviour near the free end, and the gauge interval at the center of the specimen in Specimen No.10 was *2.5D* to investigate, in detail, the bond behaviour there.

A bar was fixed centrically along a cylindrical paper form which was set vertically. The bond was removed within the region of 10*D* from the loaded end by clay and duct to avoid the influence of different confining condition near the loaded end for all the specimens except those of Series V. Unbonded region was set at the free end for Specimens No.8 and No.9 in Series I to check the similar influence at the free end. Concrete was cast in vertical direction parallel to the bar.

The apparatus for the pullout test are given in Fig.2. Axial load was applied by a center-hole jack. The direction of tensile load applied to the bar was opposite to the casting direction of concrete for both the pullout tests and the axial tension test. In addition to strains, free end slips were measured by a displacement meter and applied forces were measured by a load cell.

2.4 Determination of Local Bond Stress and Slip /6/

The strain distribution curve was obtained by connecting every three neighboring points with 2nd degree polynomial functions.

In pullout tests, the local slip is obtained by taking summation of the free end slip and the integration of strains from the free end to the point concerned. In axial tension tests, the local slip is obtained by integration of the strain from the zero-slip point to the point concerned. The zero-slip point was determined to be the point where the slope of strain distribution curve is zero. The slip is thus defined as, not relative displacement between bars and concrete, but the displacement of the bar at the point concerned from the fixed point in concrete. This definition has generality because the relative displacement between bars and concrete depends on the distance to the point concerned in concrete from the bar surface.

The local bond stress at any location along an embedded bar is thus proportional to the slope of the strain distribution curve at that point. At any point, the bond stress is expressed as $\tau = ED/4 \cdot d\varepsilon/dx$, where E is the Young's modulus of the bar. D is the bar diameter and $d\varepsilon/dx$ is the slope of the strain distribution curve.

3. BOND-SLIP-STRAIN RELATIONSHIP

3.1 Effect of Strain on Bond-Slip Relationship

It was pointed out by Yamao et al./7/ that bond-slip relationships obtained from pullout tests with long embedment were different from those obtained from tests with extremely short embedment. Likewise, Chou et al./8/ reported that bond-slip relationships in pullout specimens with short embedment depends on locations along a bar. Bond-slip relationships at different distances from the free end are shown in Fig.3. These data were at *5D*, *10D* and *15D* obtained from Specimens No.2 to No.5, No.3 to No.5 and No.4 to No.5, respectively. Data at 20*D* and 25*D* were obtained from Specimen No.5. The bond-slip relationships differ with locations along a bar and the bond stress becomes larger at the location closer to the free end.

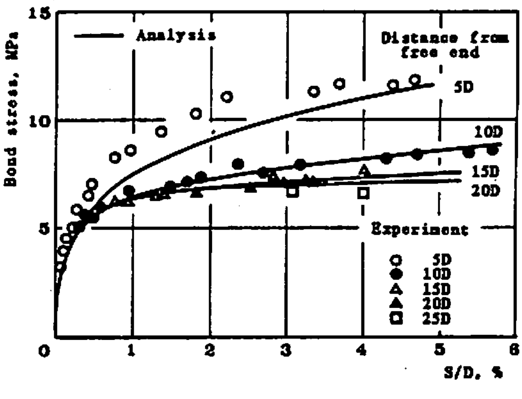

Fig.3 Bond-slip relationships at different locations along a bar in pullout test with short embedment.

There is no significant difference in bond-slip relationships among various unbonded lengths at the free end as shown in Fig.4, which shows that the bond-slip relationships at 2*D* from the free end in Specimens No.7, 8, 9 whose unbonded length at the free end were varied to be 0*D*, 2.5*D* and 5*D*, respectively.

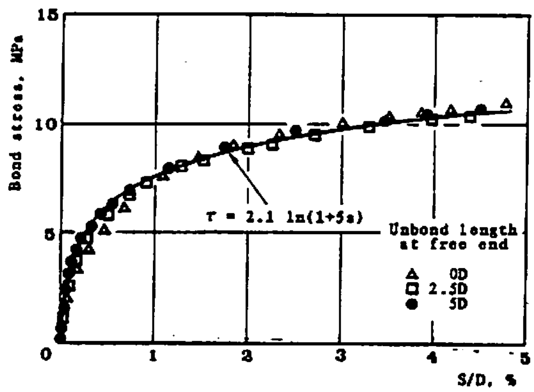

Fig.4 Bond-slip relationship at 2D from free end with various unbonded length at free end.

The experimental results of the strain distribution obtained from the axial tension test are given in Fig.5. The bond-slip relationships at different location along a bar calculated from the strain distribution is shown in Fig.6, which shows the bond-slip relationship depends on the location and the bond stress becomes smaller as the location is closer to the center of the specimens.

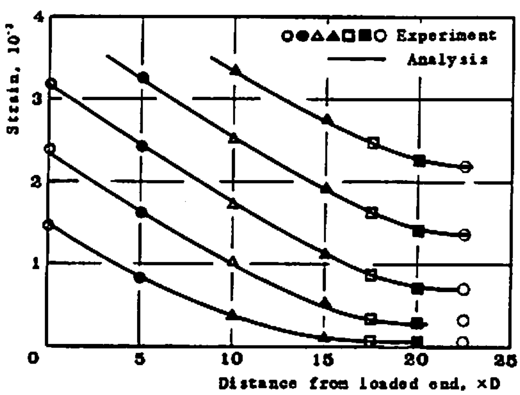

Fig.5 Strain distributions in axial tension test.

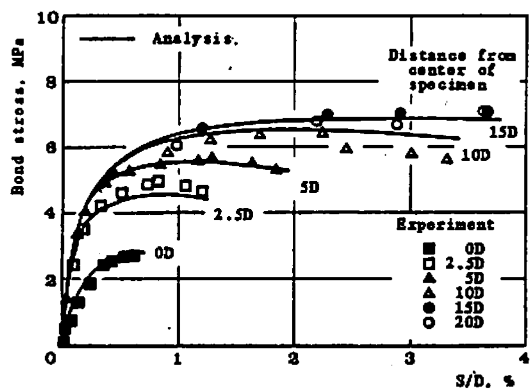

Fig.6 Bond-slip relationships at different locations along a bar of axial tension test.

Moreover, in the pullout test with long embedment, the bond-slip relationship of an aluminium bar is different from that of a steel bar. The bond-slip relationships at every measured location along the aluminium bar and the steel bar obtained from Specimens No.11 and No.12 are shown in Fig.7. As mentioned later, the bond-slip relationships at different locations along a bar are the same if the embedded length is long enough. The bond stress of the aluminium bar is significantly smaller than that of the steel bar at the same slip. This fact indicates that the difference in strain affects the bond-slip relationship.

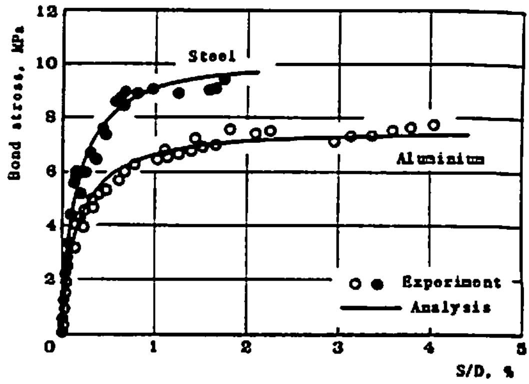

Fig.7 Bond-slip relationships of aluminium bar and steel bar.

First of all, it is postulated that the bond stress at the same slip becomes smaller when

A) the strain becomes larger or

B) the tensile stress becomes larger

regardless of the material. Then, from the comparison between the aluminium bar and the steel bar, it is assumed that the smaller bond stress of the aluminium bar is resulted from larger strain of the aluminium bar comparing with that of steel bar at the same slip as shown in the upper part of Fig.8. This means that the postulation A is used. Then the tensile stress of the aluminium bar should be smaller than that of the steel bar when the bond stress of the aluminium bar becomes smaller than that of the steel bar as shown in the bottom part of Fig.8. This indicates that the influence of stress on the bond-slip relationship is contrary to the postulation B. It is concluded that the difference of tensile stress of a bar does not affect the bond-slip relationship or the influence of tensile stress is quite smaller than that of strain. It may be doubtful if the corrosion affects the lower bond stress of the aluminium bar. However, the material made by the corrosion around the aluminium bar embedded in concrete is precise and very thin/9/. Furthermore, the same equation of the effect of strain on bond stress holds good in both the aluminium bar and the steel bar as mentioned later. Therefore, there is no effect of corrosion or lower hardness of aluminium on the lower bond stress.

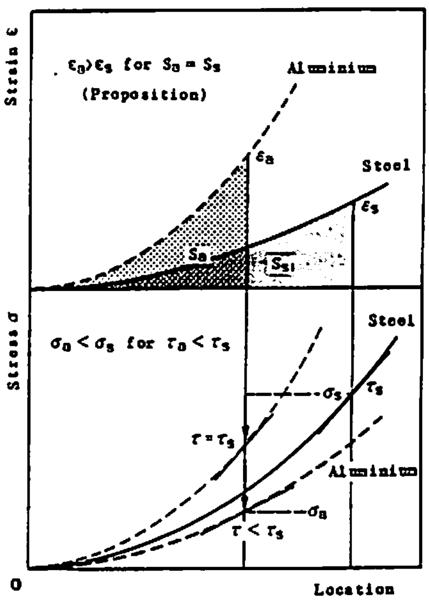

Fig.8 Strain and stress distributions of aluminium bar and steel bar.

The local difference of bond-slip relationship of the steel bar in the case of pullout specimens with short embedment and axial tension specimens can be expressed by the concept of the effect of strain on the bond-slip relationship. In the pullout specimens, when the free end slip occurs, that is the zero strain with the non-zero slip, the strain of the bar corresponding to a certain slip becomes smaller and finally the bond stress becomes larger near the free end. Conversely, in the axial tension specimen, the strain of a bar increases regardless of zero slip at the center of the specimen. The strain of the bar corresponding to a certain slip becomes larger near the center of the specimen and finally the bond stress becomes smaller.

Therefore, it is considered that the differences in bond-slip relationship mentioned above can be expressed by using an unique bond-slip-strain relationship.

3.2 Formulation of a Bond-Slip-Strain Relationship

In order to formulate a bond-slip-strain relationship which holds good under any boundary conditions and materials, the following form is introduced to express the bond stress τ by the function of slip S and strain ε.

$$\tau = \tau_0 \cdot g(\varepsilon) \tag{1}$$

where the bond stress τ_0 is the one that is a function of slip when the strain is zero, and the function $g(\varepsilon)$ expresses the effect of strain.

These functions are impossible to be obtained directly from experimental results. Among the experiments, the closest function for τ_0 is the bond-slip relationship at $2D$ from the free end of Specimens No.7 to No.9 with extremely short embedment as shown in Fig.4. Here, we have to pay attention to the effect of concrete strength. Because the strain at a certain slip becomes larger for long embedment specimens when the concrete strength becomes higher due to the larger bond stress. Therefore, the effect of concrete strength must become larger than that in a long embedment specimen.

The effect of concrete strength in zero-stress was determined from the relationship between the concrete strength and the average bond stress at sufficiently large slip compared with the strain as shown in Fig.9. This was obtained from extremely short embedment specimens No.13 to No.15 whose strains were small compared to the slips. The effect of bar diameter is also considered by using non-dimensional slip $s=1000S/D$, where S is slip and D is bar diameter, because the slip is proportional to the bar diameter/7,10/.

$$\tau_0 = f'_c \cdot f(s)\,. \tag{2}$$

When the bond stress is proportional to the concrete strength in case there is no influence of strain on the bond-slip relationship, the bond stress τ_{2D} at $2D$ from the free end shown in Fig.4 is expressed as

$$\tau_{2D} = 2.1 \cdot \ln(1+5s) \quad \text{(MPa)} \tag{3}$$

where $s=1000S/D$. Using this relationship, the bond stress τ_0 is assumed as expressed by

$$\tau_0 = f'_c \cdot k \cdot (\ln(1+5s))^c \quad \text{(MPa)} \tag{4}$$

where k and c are constants.

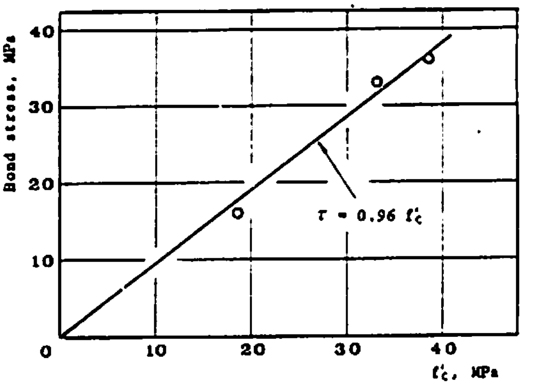

Fig.9 Relationship between concrete strength and bond stress when strain is small compared to slip.

From Eq.(1) and Eq.(4), we express the function of $g(\varepsilon)$ as

$$k \cdot g(\varepsilon) = \frac{\tau}{f'_c(\ln(1+5s))^c}\,. \tag{5}$$

The function $g(\varepsilon)$ can be obtained by plotting strains on the x axis and computed values from the right-hand side of Eq.(5) on the y axis, as we know that the slip and strain corresponding to a certain bond stress are given by experiment. The most suitable value for the constant c is determined by making the function to be expressed by an unique equation in spite of materials and boundary conditions. After many trials we decided to three to be the most suitable value for the constant of c. It is shown in Fig.10 that the function becomes unique for the constant c of 3 in case of the steel and aluminium bar. Then, the constant k becomes 0.73 and the bond stress τ_0 is finally represented by

$$\tau_0 = 0.73(\ln(1+5s))^3 f'_c \quad \text{(MPa)}. \tag{6}$$

From Eq.(1) and Eq.(6), the function $g(\varepsilon)$ is expressed by

$$g(\varepsilon) = \frac{\tau}{\tau_0} = \frac{\tau/f'_c}{0.73(\ln(1+5s))^3}. \tag{7}$$

In Fig.11 and Fig.12, the reciprocals of Eq.(7) for the specimens having different bond-slip relationships are demonstrated, Fig.11 for the boundary condition of non-zero strain with zero slip in specimen No.10 and Fig.12 for the steel and the aluminium bar. As shown in these figures, all data can be expressed by an unique bond-slip-strain relationship and then the function $g(\varepsilon)$ can be expressed by

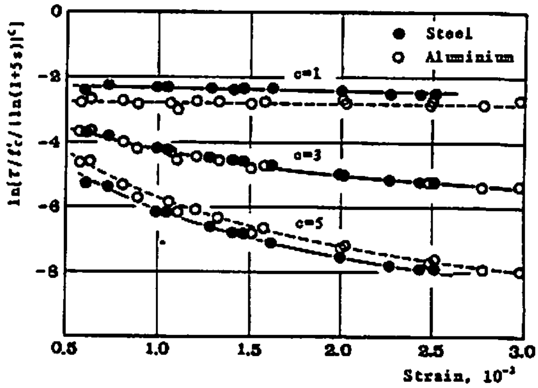

Fig.10 Variances of k g(ε) with different "c" of aluminium bar and steel bar.

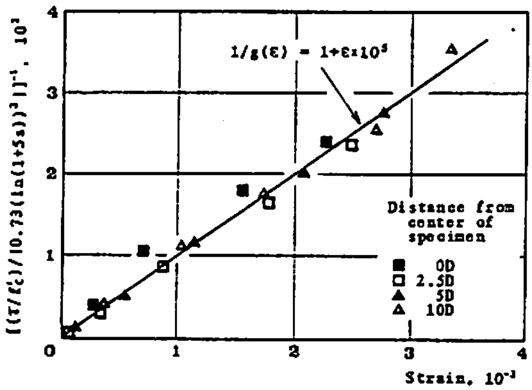

Fig.11 Bond-slip-strain relationship under boundary condition of non-zero strain with zero slip.

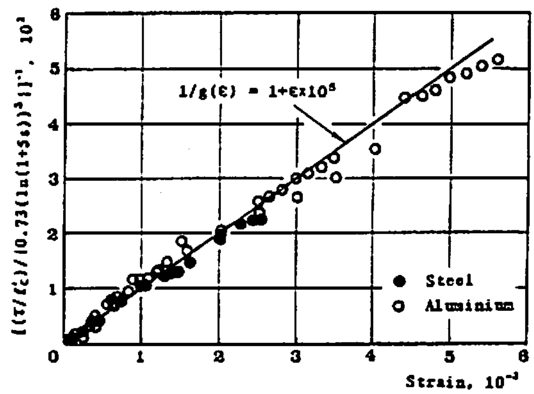

Fig.12 Bond-slip-strain relationship of aluminium bar and steel bar.

$$g(\varepsilon) = \frac{1}{1+\varepsilon\times 10^5}. \tag{8}$$

Finally, from Eq.(1), Eq.(6) and Eq.(8), the bond-slip-strain relationship can be expressed as

$$\frac{\tau}{f'_c} = \frac{0.73(\ln(1+5s))^3}{1+\varepsilon\times 10^5}. \tag{9}$$

where s=1000S/D, τ: bond stress, f'_c: concrete strength, S: slip, D: bar diameter, ε: strain. Units are same for the bond stress and the concrete strength as well as those for the slip and the bar diameter. Fig.13 reveals the bond-slip-strain relationship by means of the effect of strain on bond-slip relationship.

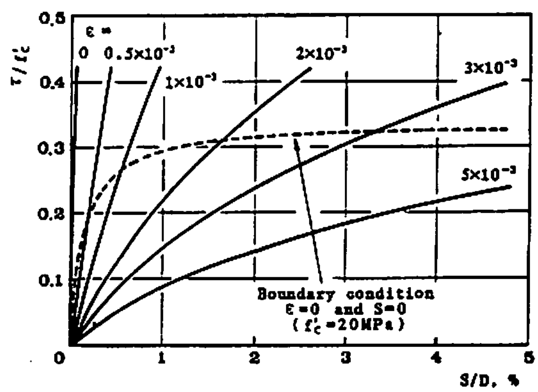

Fig.13 Calculated bond-slip-strain relationship expressed by effect of strain on bond-slip relationship.

The different bond-slip relationships resulting from the different boundary conditions and Young's modulus can be calculated backward from this bond-slip-strain relationship. These are shown in Fig.3,

Fig.6 and Fig.7. These figures clearly indicated that the bond-slip relationships under various conditions can be expressed by the unique equation of bond-slip-strain relationship.

In order to verify the accuracy of measured strain distributions under three different boundary conditions, non-zero strain with zero slip, zero strain with zero slip and zero strain with non-zero slip are compared with those calculated from the bond-slip-strain relationship as shown in Fig.5, Fig.14 and Fig.15, respectively. The analytical results agree well with the experimental results. The bond-slip-strain relationship expressed by Eq.(9) has high accuracy under all different conditions.

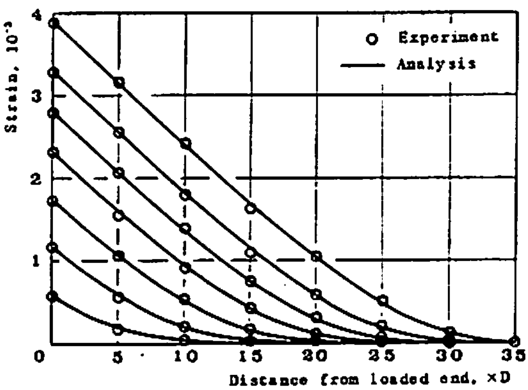

Fig.14 Strain distribution of Specimen No.6 under boundary condition of zero strain with zero slip.

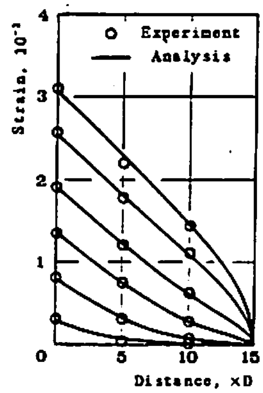

Fig.15 Strain distribution of Specimen No.3 under boundary condition of zero strain with non-zero slip.

The bond tests carried out by other investigators can be simulated if confining condition of concrete is similar. The experiments of Hawkins et al./5/ and Mirza and Houde/3/ are shown in Fig.16 compared with the calculated results. Hawkins et al. carried out the pullout tests with embedment length from 1 rib to 4 ribs under the condition of well-confined concrete, causing no occurrence of splitting cracks, and proposed the bond-slip relationship obtained from the average bond stress. Mirza and Houde proposed the bond-slip relationship obtained from axial tension tests with short embedment. Although these two relationships are very different, the bond-slip-strain relationship can express the both.

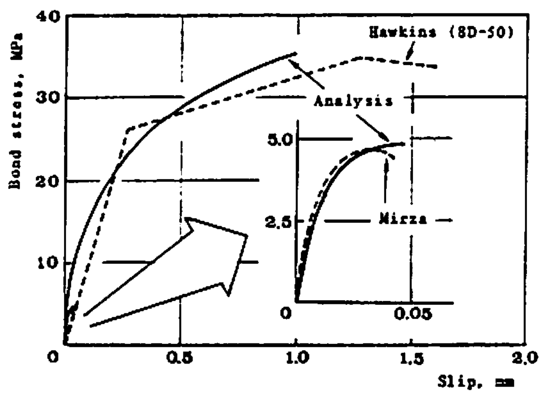

Fig.16 Simulation of Hawkins'/5/ and Mirza's/3/ experiments using bond-slip-strain relationship.

4. BOND-SLIP RELATIONSHIP IN LIMITED CONDITION AS LONG EMBEDMENT

In the limited condition that the embedded length is long enough, in which the condition is always that the strain equals to zero where the slip is zero or the slip equals to zero where the strain is zero, the strain distribution curves at any loading step are supposed to be made by parallel translations of an unique curve in direction along the bar. This means that the three factors of bond stress, slip and strain have an unique relationship among them. Then, the bond- slip relationship can be represented by an unique relationship, because the strain at a certain point along a bar is not independent on the bond stress or the slip.

5. BOND-SLIP RELATIONSHIP IN POST-YIELD RANGE OF STEEL

The authors/11/ investigated the bond characteristics in post-yield range of deformed bars by means of the similar pullout tests with long embedment using different strength bars. It was clarified that the bond stress in post-yield range was much lower than that in elastic range and decreased suddenly with the yielding of steel. Also it was reported that the bond-slip relationship in post-yield range depended on the stress-strain properties of a bar characterized by yield strength, length of yield plateau and stiffness in strain hardening range. According to the bond-slip-strain model, stress, strain and stiffness of a steel bar at a certain slip should be dependent on the stress-strain properties of the bar, and is considered to be applicable to the post-yield range.

The bond-slip relationships of specimens SD35(yield strength f_y=350MPa, initial strain of strain hardening ε_{sh}=1.65%), SD50(f_y=610MPa, ε_{sh}=1.40%) and SD70(f_y=820MPa, ε_{sh}=0.60%) are shown in Fig.17. The bond-slip relationship is independent on the locations along a bar in case of the condition that the slip is zero where the strain is zero. The analytical bond-slip relationships using the bond-slip-strain relationship are added to Fig.17. The analytical results agree well with the experimental results. The analysis using the bond-slip-strain relationship expresses the variance of the slip at yielding and the bond-slip relationship in post-yield range with the difference of properties of steel.

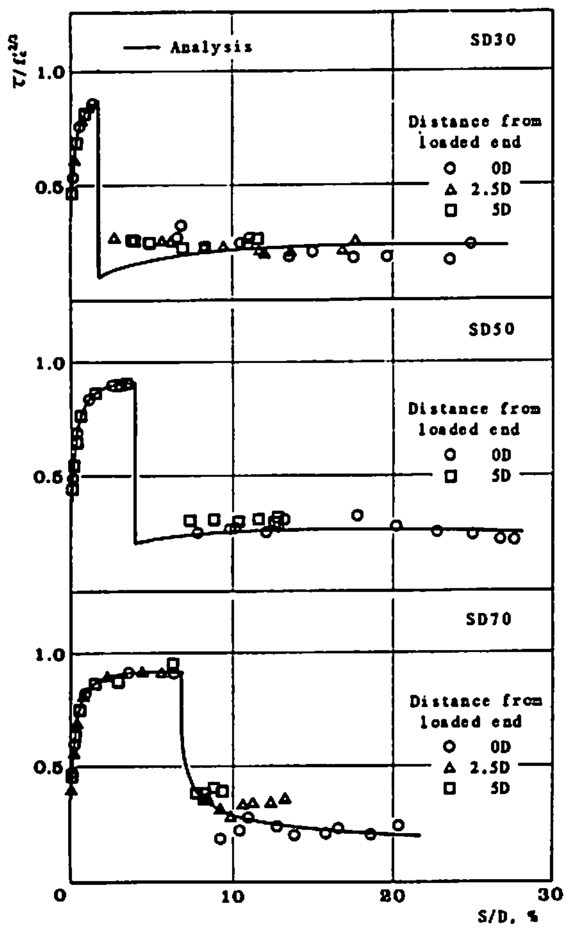

Fig.17 Bond-slip relationships including post-yield range.

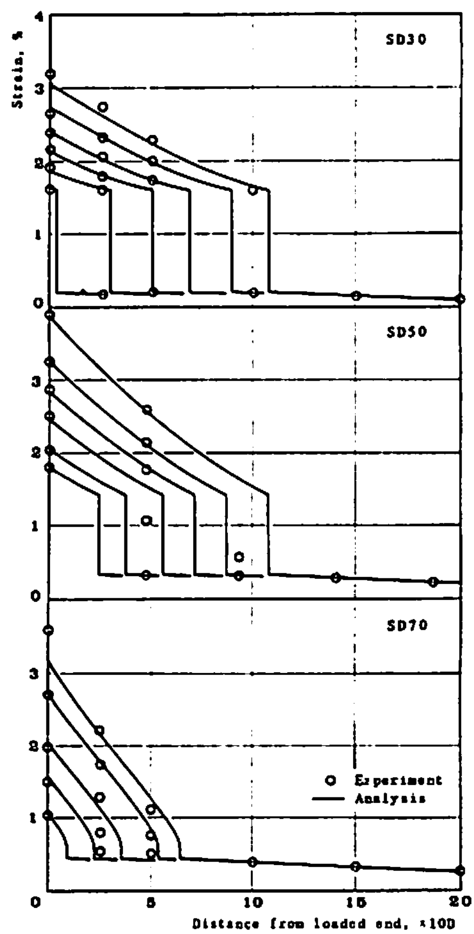

Fig.18 Strain distribution in post-yield range.

In order to verify the accuracy of the bond-slip-strain relationship, the experimental results measured directly from the tests are compared to those calculated using the bond-slip-strain relationship. Fig.18 shows the comparison of the analytical strain distribution with the experimental results. It is indicated that the accuracy is good. In conclusion, the bond-slip-strain relationship has good accuracy even in the post-yield range of steel.

6. CONCLUSIONS

(1) The bond-slip relationship depends on the location along a bar when the boundary condition is that the strain is zero where the slip is not zero, or the strain is not zero where the slip is zero.

(2) The bond-slip relationship of an aluminium bar which has smaller Young's modulus than steel is different from that of a steel bar.

(3) The experimental facts described in (1) and (2) can be explained by the analysis using the proposed bond-slip-strain relationship, formulated considering the effect of concrete strength and bar diameter.

(4) The proposed bond-slip-strain relationship is applicable to post-yield range of steel. The complicate bond-slip relationships in post-yield range can be expressed by the analysis using the unique bond-slip-strain relationship.

(5) The bond stress can be expressed by a function of only the slip in case of the condition that the strain is zero where the slip is zero.

REFERENCES

/ 1/ H.Muguruma, S.Morita and K.Tomita, "Fundamental Study on Bond between steel and concrete," Trans. of AIJ, No.131, Jan.1967, pp.1-8, No.132, Feb.1967, pp.1-6 (in Japanese).

/ 2/ S.Morita and T.Kaku, "Local Bond Stress-Slip Relationship under Repeated Loading," Preliminary Report, IABSE Symposium, Lisbon, 1973, pp.221-227.

/ 3/ S.M.Mirza and J.Houde, "Study of Bond Stress-Slip Relationships in Reinforced Concrete," ACI Journal, Jan. 1979, pp.19-46.

/ 4/ V.Ciampi, R.Eligehansen, V.Bertero and E.Popov, "Analytical Model for Deformed Bar Bond under Generalized Exitations," IABSE Colloquium Delft 1981, Report of the Working Commissions, vol.34, IABSE, pp.53-67.

/ 5/ N.M.Hawkins, I.J.Lin and F.L.Jeang, "Local Bond Strength of Concrete for Cyclic Reversed Loadings," Bond in Concrete, Proceedings of the International Conference on Bond in Concrete, Applied Science Publishers, London, 1982, pp.151-161.

/ 6/ A.H.Nilson, "Internal Measurement of Bond Slip," ACI Journal, July 1972, pp.439-441.

/ 7/ H.Yamao, L.Chou and J.Niwa, "Experimental Study on Bond stress-Slip Relationship," Proc. of JSCE, No.343, 1984, pp.219-228 (in Japanese).

/ 8/ L.Chou, J.Niwa and H.Okamura, "Bond Model for Deformed Bars Embedded in Massive Concrete," Proc. of 2nd JCI Colloquium on Shear Analysis of RC Structures, JCI, 1983, pp.45-52 (in Japanese).

/ 9/ Y.Takatani, K.Yamakawa and S.Yoshizawa, "Effect of Sodium Choloride on Corrosion of Aluminum Alloys Burried in Mortar and Concrete," Journal of the Society of Materials Science, Japan, Vol.35, No.398, 1986, pp.1310-1315 (in Japanese).

/10/ S.Morita and S.Fujii, "Bond-Slip Models in Finite Element Analysis," Proceedings of Japan-US Seminar on Finite Element Analysis of Reinforced Concrete Structures, Tokyo, May 1985, ASCE, pp.348-363.

/11/ H.Shima, L.Chou and H.Okamura, "Bond Characteristics in Post-Yield Range of Deformed Bars," Concrete Library International, No.10, JSCE, 1987, pp.113-124.